Improving cost effectiveness in additive manufacturing – Increasing dimensional accuracy in laser beam melting by means of a simulation-supported process chain

Fabian Bayerlein[a], Christian Zeller[a], Michael F. Zäh[b], Johannes Weirather[a], Martin Wunderer[a], Christian Seidel[b]

[a]Institute for Machine Tools and Industrial Management (iwb), Application Center Augsburg, Technische Universität München, Germany
[b]iwb, Technische Universität München, Germany

Summary

With the increasing use of laser beam melting (LBM) in the industrial manufacturing process and its increasing stability, cost effectiveness is gaining more and more attention. However, due to process inherent, temperature related strains, warpage is induced and the dimensions of the final part are frequently outside the allowed tolerance. Currently, this challenge is met by manually adjusting the design of the part, its orientation on the build platform or the support structure. In this manuscript, a novel approach based on a simulation-supported process chain is presented. By pre-warping the input shape and re-simulating the manufacturing process in an iterative manner, the output shape converges to a result with minimal distortion compared to the initial design.

Keywords

Additive Manufacturing, Laser Beam Melting, warpage, distortion, simulation, FEA (Finite Element Analysis), Inconel718

1. Introduction

Laser beam melting (LBM), part of the rapidly emerging additive manufacturing (AM) sector, is a metal-based process for the creation of three-dimensional parts. In contrast to conventional machining, like turning or milling, where material is removed in order to reach the target shape, during an LBM process, said shape is generated by adding layer upon layer in the build-up direction. The individual layers consist of small laser welded seams, which are overlapping with each other and the previous layers, creating a coherent solid body with the desired geometry. Different forms of the source material like wires, powders and liquids are used throughout the AM technologies. The powder-based LBM process is used in a variety of industry sectors, including aerospace and dental technologies for example.

With the recent transition of AM processes from the prototyping into the manufacturing domain, the requirements in terms of dimensional accuracy and part durability are increasing. However, the main economic potential for AM resides in small production lots of parts with highly complex geometry. In these cases, missing predictability of the process-inherent warpage, especially for complex geometries, poses a considerable challenge [1]. To avoid these dimensional deviations in the final product, different remediation measures can be employed. The most commonly used procedure is an iterative, experimental trial-and-error approach. By changing the design of the part or its orientation on the build platform as well as the support structure and rebuilding the part, the resulting warpage is reduced in a stepwise manner. The number of iterations needed to satisfy the requirements depends on the user's experience and process know-how. Additionally, each iteration does not only comprise the expensive manufacturing step but also a diligent determination of dimensional deviations.

In this manuscript, a simulation-based process chain is presented, that also targets to minimize dimensional deviations, but prior to the actual AM process resulting in a possibility for substantial economic benefits. The corresponding simulation model is explained in detail in section 2. The suggested pre-warping algorithm and its implementation are presented in section 3. Lastly, section 4 summarizes the benefits of the developed strategy and presents future research objectives.

2. Simulation model

In order to model the transient process of LBM, abstractions are necessary to allow for numerical simulation within reasonable time. The object of interest, the resulting warpage of the part, is caused by thermal strains due to the laser's localized energy input. An in-depth description of the used simulation model respecting the explained requirements is given in [6]. Key elements are explained as needed.

2.1 Modelling approach

One important characteristic of powder-based LBM is the manufacturing of parts by adding distinct layers of material. To enable a realistic simulation of resulting residual strains and warpage of the part, this structure is transferred to the Finite Element Mesh by restricting the position of the nodes in build-up direction to discrete levels. With real parts comprising thousands of layers, abstractions are made by summarizing multiple real layers in so-called layer compounds (LC). Additionally, while the real process involves sequential melting of powder in a hatch-wise manner, the simulation simplifies the heat input to a simultaneous application on the whole layer, i. e. a layer compound [12].

The thermal and mechanical simulation are sequentially coupled by solving the transient heat equation and applying the calculated temperature distribution per time step as distinct load steps in the mechanical simulation. The feedback of the resulting warpage is deemed negligible for the thermal simulation due to its limited effect size.

To generate the mesh for the simulation, two different strategies are implemented within the presented simulation model. Within the machine-data (CLI) based approach, keypoints according to the scan strategy are created, which in turn create areas. The areas are meshed with quads and extruded in build-up direction, resulting in multiple 3-dimensional hex-meshes, which are coupled by constraint equations [6]. The other approach uses standard CAD-data for mesh creation. The first step is slicing the volume into layers with a custom program. Then, the layered geometry is meshed in ANSYS Workbench, creating a coherent mesh with nodes lying at distinct levels in build-up direction. Hexahedron as well as tetrahedron elements can be chosen, allowing more flexibility for the user. A different meshing strategy is presented by [2], where the part is meshed by superimposing a 3-dimensional grid and a subsequent rearrangement of the nodes.

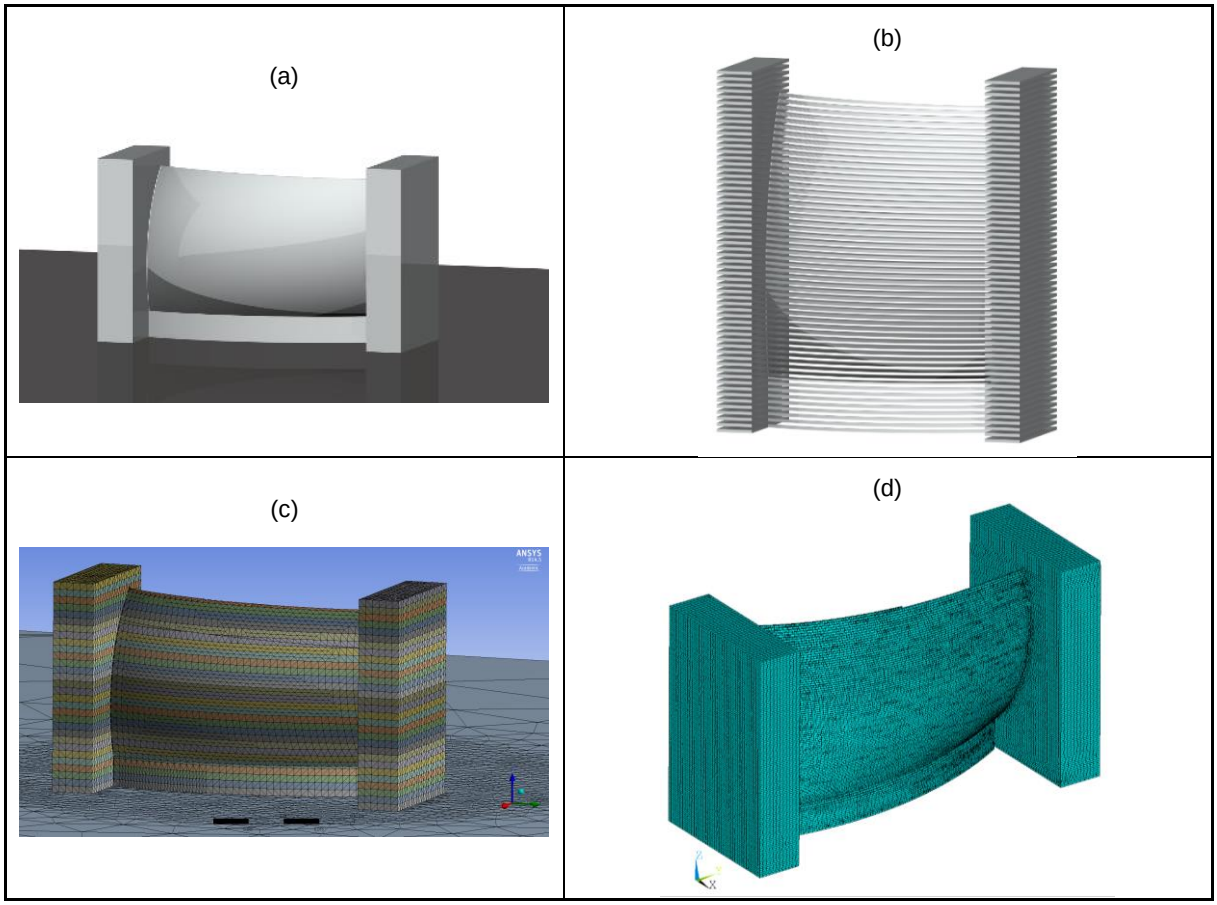

Figure 1: Overview of the CAD-based meshing procedure and comparison to the (d) CLI-based mesh: (a) CAD Model of the turbine blade geometry on the build plate, (b) extruded view of the separated volumes after the slicing process, (c) layer-wise, coherent mesh created with ANSYS Workbench

Similar to the real process, its simulation is conducted in a layer-wise fashion. At the beginning, all elements forming the part are deactivated and only the build plate and the pre-heating platform are active. During the simulation layers are sequentially activated, heat load is applied and the cooling-off phase is simulated. The load is applied by means of a temperature constraint with the value of the solidus temperature of the respective material. The load-time for the temperature-based heat generation model is calculated by the ratio of the melt-pool length and the scan velocity of the laser spot. The mentioned approach is presented in [3]. Here, the melt pool length is determined by Rosenthal's solution for moving heat sources on a semi-infinite body [13]. Subsequently, the constraints are deleted and the cooling phase is initiated, allowing the model to simulate the heat flow responsible for the formation of tensions and plastic strains that cause residual stress and warpage [6].

Additionally, for achieving reliable simulation results the quality of the material data is of importance. The parameters influencing the thermal calculation are density ρ, specific heat capacity c and thermal conductivity λ [9]. Thus, the thermal diffusivity is defined as

$$\alpha(T) = \frac{\lambda(T)}{\rho(T) \cdot c(T)}. \tag{1}$$

The heat conduction equation is a quasilinear differential equation. This stems from the fact, that the material parameters are functions of the temperature. They are often assumed to be constant for small temperature ranges, so that the system is simplified to a linear set of differential equations. During the Laser Beam Melting process temperatures between room temperature and the melting point of the metal occur. Hence, the approximation of temperature-independent material parameters is not suitable here. The mechanical calculation is influenced by Young's modulus E, thermal strain α and Poisson's ratio ν. Analogous to the thermal material data the mechanical material parameters can neither be assumed to be constant. The thermo-physical and thermomechanical data were obtained by own measurements

and are in good accordance with the data presented in [8]. Table 1 shows an overview of the material properties used within the simulation.

Table 1. Temperature dependent material properties of Inconel 718

	20 °C	1255 °C	Units
Thermal			
Thermal conductivity λ	10	30	$W/(m \cdot K)$
Specific heat capacity c	430	650	$J/(kg \cdot K)$
Mechanical			
Thermal strain α	0	0,023	mm

During Laser Beam Melting compressive stresses can occur both in the base plate and the part. During the manufacturing process, a conversion from compressive to tensile stresses can be observed in several regions (plate and part). For considering the relating load inversion the elastic-plastic material behavior is modelled by kinematic hardening.
The heat conduction equation is a parabolic differential equation. So the initial values and boundary values have to be set adequately. The observed volume is represented by the set $\Omega \subset \mathbb{R}^3$ with the composed set Γ as boundary condition. The latter consists of the regions Γ_{Top}, the interface to the powder bed Γ_{Powder}, the surface of the base plate $\Gamma_{Substrate}$ and the underlying pre-heating plate $\Gamma_{Pre-Heating}$.

$$\Gamma = \Gamma_{Top} \cup \Gamma_{Powder} \cup \Gamma_{Substrate} \cup \Gamma_{Pre-Heating} \tag{2}$$

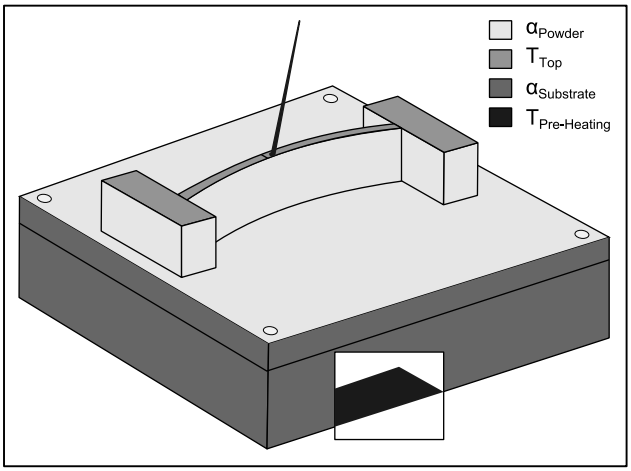

Figure 2: Boundary conditions set during the heating phase. Fixed temperatures are applied at the top of the part and the bottom of the pre-heating platform and convective loads are applied on the substrate, pre-heating platform and all surfaces in contact with powder.

On both sets Γ_{Powder} and $\Gamma_{Substrate}$ convective boundary conditions are established. Due to very limited impact on the results, the area contacting the powder Γ_{Powder} is frequently assumed to be adiabatic [10]. In the region $\Gamma_{Pre-Heating}$ a constant temperature is present. The boundary condition Γ_{Top} is changed from a fixed temperature value in the heating phase to a convective boundary condition during cooling-off.

As mentioned earlier, the results from the transient thermal simulation (i. e. the temperature field) are used as a load for the following mechanical simulation. As the model considers plasticity, it exhibits the characteristic of a non-conservative system. Therefore, the sequence of load steps within the mechanical simulation needs to be equivalent to the one within the thermal simulation.
The screws clamping the base plate are modelled by a fixation of the degrees of freedom of the drill holes. It is necessary for achieving the goal of acceptable computation times to keep the amount of time steps as low as possible. Simultaneously the temperature field must contain sufficient information for the computation of the residual stresses and distortions occurring as a result of temperature gradients. Hence, the ANSYS algorithm for automatic time-stepping is used. In this regard, it has to be considered, that the first two time steps have constant values and the adaptive time stepping starts with the third step.

2.2 Validation of the model

To validate the developed simulation model, different studies were conducted. Besides dimensional deviations, also comparisons of the residual stress state between the simulation and the actual manufacturing process are examined. A standing brick geometry (40x10x40 mm, with z aligned to the build-up direction and reaching 40 mm and x along the longer edge) was chosen as a first validation example. The Inconel 718 part was manufactured on an EOS M280-system at MTU Aero Engines AG with standard parameters. The experimental values were gathered by means of neutron diffraction at the STRESS-SPEC instrument of the Heinz Maier-Leibnitz Zentrum in Garching, Germany. The lattice strain of the {311} Nickel plane in reference to a stress-free reference sample was used for all measurements. Preliminary results show good agreement between experimental and numerical results. With the neutron measurements being very susceptible to errors in the stress-free reference sample, additional hole drilling trials will confirm these results. However, the findings are consistent with [5].

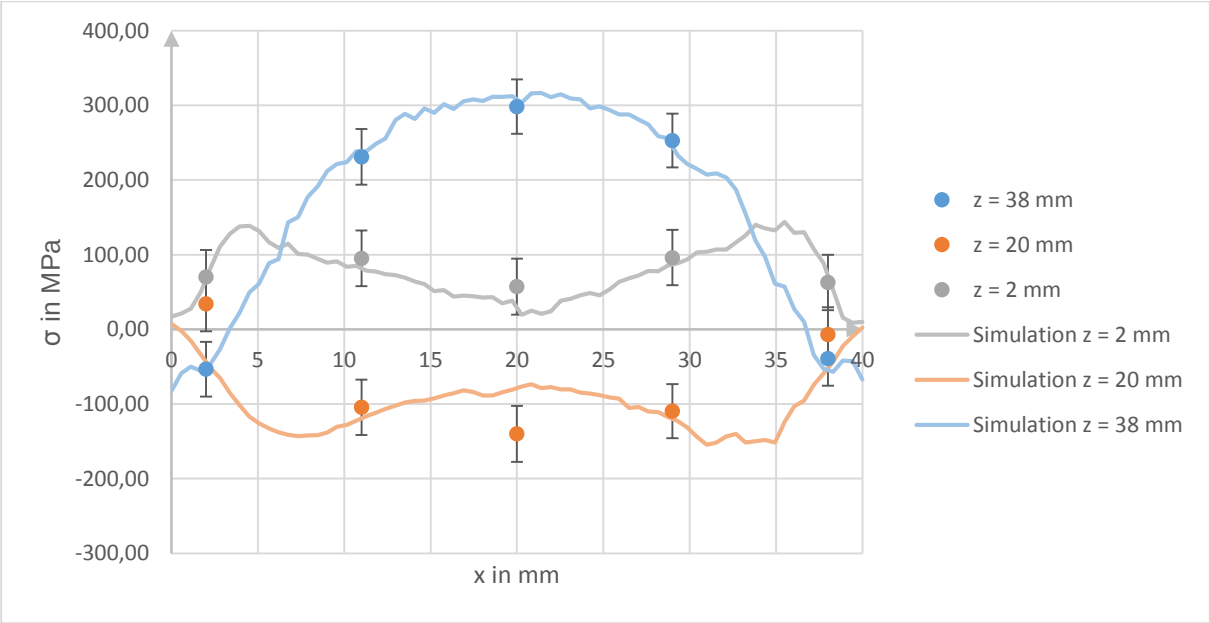

Figure 3: Residual stresses in a standing brick geometry for three different levels of z, i. e. the build-up direction. The measured values in the actual sample are provided as a dot and the respective error bars represent the uncertainty of the peak fit of the diffractometry data. The continuous lines are extracted from the simulation by averaging over all nodal values within a sample volume comparable to that of the neutron diffractometry experiments.

3. Pre-warping

The concept of pre-warping the part to compensate for the resulting dimensional deviations is well-established in non-metal and metal based additive manufacturing, whether this results from process or machine specific factors [4, 7]. In most cases, this pre-warping process involves multiple manufacturing steps and respective measurements of distortions. The corresponding convergence and duration depend on the experience of the user and the availability of the technical equipment. Another possibility is to substitute the actual build-up step for a manufacturing simulation, establishing the transition to a simulation-supported process chain. Commonly, this method involves a single-stage adjustment of the input CAD-file by inverting the warpage results of the manufacturing result, i. e. the dimensional deviations. However, the non-linear manufacturing process is not likely to yield the desired geometry at the first iteration. To facilitate the distinction between the different domains, all manufacturing related quantities are tagged with a circumflex (e. g. $\hat{y}$) and all those related to simulation with a tilde (e. g. $\tilde{y}$). To further the assistance of the simulation to the AM user, an iterative approach to minimize dimensional deviations is investigated. Additionally, a simulation-supported process is only viable if the designated user's abilities are coherent with the requirements of the described process, creating a need for automatization.

In order to meet these requirements, an automated process for the iterative simulation and pre-warping of laser beam melting is implemented. The underlying method of iteratively improving the solution is based on a fix point iteration according to the following rationale. The additive manufacturing process

can be interpreted as a function $f: \mathbb{R}^3 \rightarrow \mathbb{R}^3$, with the resulting position vector $y \in \mathbb{R}^3$ generated from the input, i. e. the desired vector, $x \in \mathbb{R}^3$.

$$f(x) = y \tag{3}$$

Due to process-inherent strains, warpage results and the corresponding geometries mismatch

$$x \neq y. \tag{4}$$

To compensate for this warpage, an input geometry x_{opt} is to be determined, so that the manufacturing result matches the input geometry.

$$f(x_{opt}) = y_{opt}. \tag{5}$$

To reach x_{opt}, an iteratively improved solution x_i is generated by adding the difference between desired and actual warpage to the initial pre-warped geometry. For $i = 1,2, \ldots$ and $x_0 = y_{opt}$ this means:

$$\Delta x_i = f(x_{i-1}) - y_{opt} \tag{6}$$

$$x_i = x_{i-1} - \Delta x_i \tag{7}$$

To verify this approach, eq. 3 is written as:

$$f(x_{opt}) - y_{opt} = 0. \tag{8}$$

This zero point problem is expected to be non-linear due to the assumed non-linearity of f. As there is no analytical solution to these equations in general, iterative approaches like Newton-Raphson are applied. However, those methods still require explicit knowledge of the function f. By transforming eq. 8 into an equivalent fix point equation:

$$x = g(x), \quad g: \mathbb{R}^3 \rightarrow \mathbb{R}^3, \tag{9}$$

a sequence of improved solutions $\{x_i\}$ can be generated by defining

$$x_{i+1} = g(x_i). \tag{10}$$

In this way, without knowledge of the function $g(x)$, the pre-warping process is interpretable as a fix point iteration according to

$$g(x) := x + y_{opt} - f(x). \tag{11}$$

Note that the converged solution of both the machine ($\hat{y}_{opt}$) and the simulation-based ($\tilde{y}_{opt}$) process chain are not necessarily identical to the actual optimal solution (y_{opt}), having no deviations from the original input geometry (cf. Figure 4). Ultimately, at this point, it is not yet known, whether this solution exists at all due to the non-linearity of the manufacturing process.

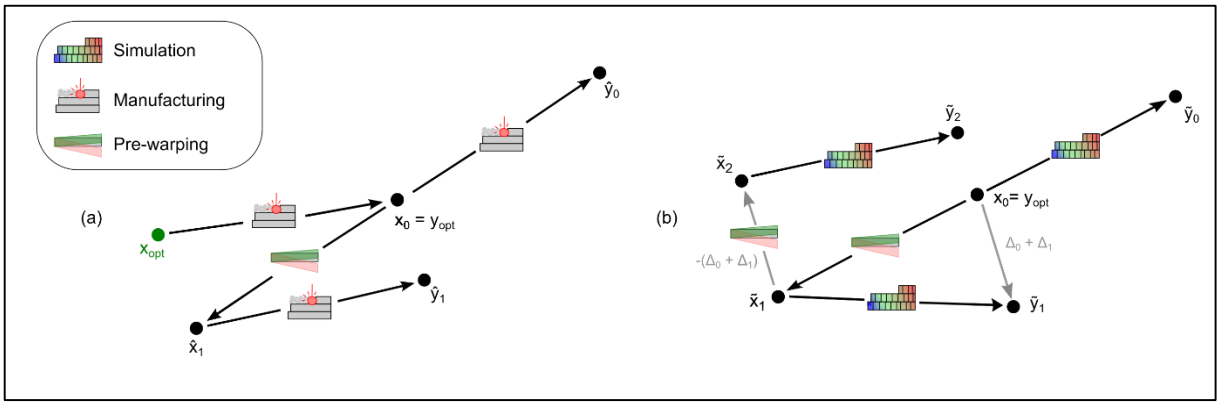

Figure 4: (a) Schematic overview of a single stage pre-warping process. With the manufacturing process being non-linear, a difference between the optimal and the manufactured part's dimensions remains. (b) Pre-warping process within the simulation. Two exemplary iterations for the presented approach are depicted.

Figure 5 presents exemplary results of the simulation-based pre-warping process. The first manufacturing simulation (Iteration 0) reveals significant dimensional deviations from the input geometry. For this simple geometry, the second iteration already results in a significant decrease of the dimensional deviations.

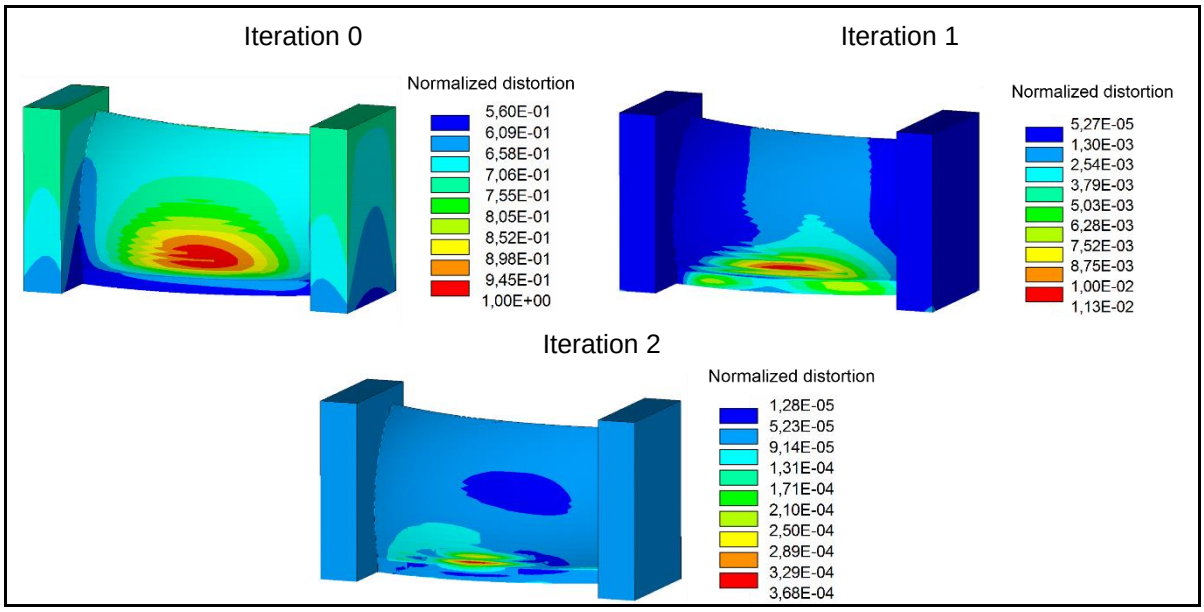

Figure 5: Development of the simulated dimensional deviations of the built-up part over the course of the iterations. The given distortion is normalized by the maximum deviation of the first simulation (Iteration 0).

The presented process is implemented in ANSYS with the help of APDL macros and only the initial, mesh is used for the simulation. Upon termination of the *n*-th simulation run, the initial mesh is distorted according to the previously mentioned pre-warping logic and then used as input for the subsequent run. This consistent mesh facilitates further processing. The error resulting from the distorted level of heat application (cf. Figure 6) is deemed negligible due to the limited size of the distortions in proportion to the height of the layer compounds.

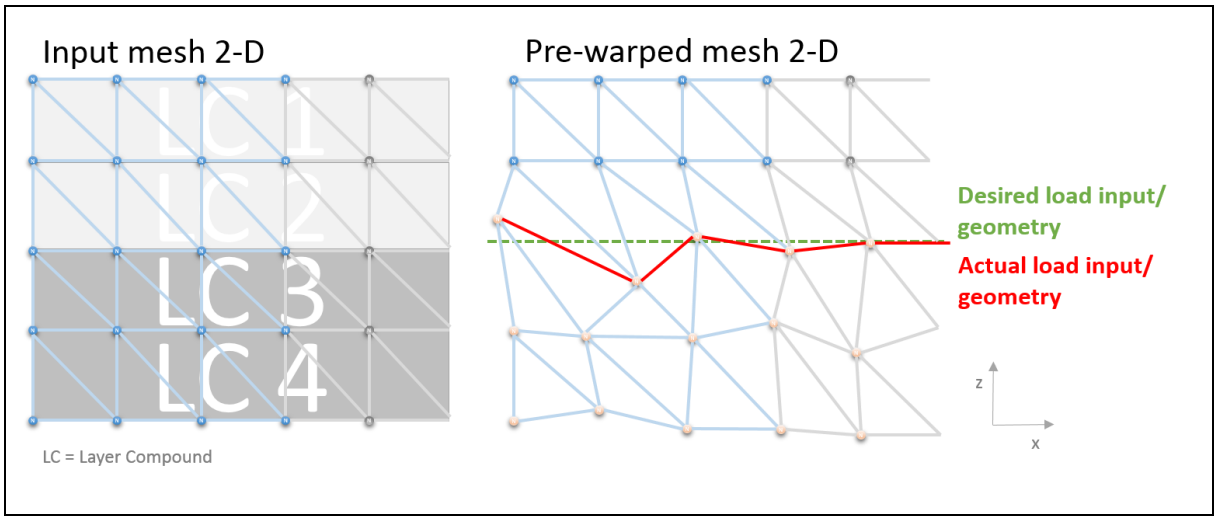

Figure 6: Comparison of desired versus actual z-level of heat input for a pre-warped mesh. Four layer compounds are shown and the proportions are exaggerated to visualize the effect.

To allow for better monitoring of the presented process, the functionality provided by ANSYS was enhanced by calculating and displaying distortions with respect to the initial rather than the input design. This enables users to quickly evaluate and confirm the effectiveness of the pre-warping process step-by-step up to the final design suggestion. Additionally, it is possible to directly extract an STL file of the pre-warped geometry for a streamlined manufacturing process.

4. Conclusion

With respect to the currently employed machine-based process chain for reaching the goal of manufacturing parts without dimensional deviations by laser beam melting, the presented approach includes significant economic advantages. The extensive work for manufacturing, measuring and manually optimizing the input geometry requires not only expertise and experience of the user as well as a longer processing time, but is also dependent on costly machinery. With all companies maximizing machine occupancy, especially for expensive equipment, delays within the machine-based process chain are likely to occur. In contrast, within the presented automated process chain, user interaction is limited to providing the correct input files. Additionally, the simulation is less time consuming, e. g. the simulation for the sample part was completed in less than two days (cf. Figure 7). With the continuous improvement of powerful simulation tools such as ANSYS and the steady improvement of computer hardware, the time consumption of such simulations will further decrease. Lastly, simulations are expected to be less cost-intensive as total costs are dominated by costs for licenses and PC hardware.

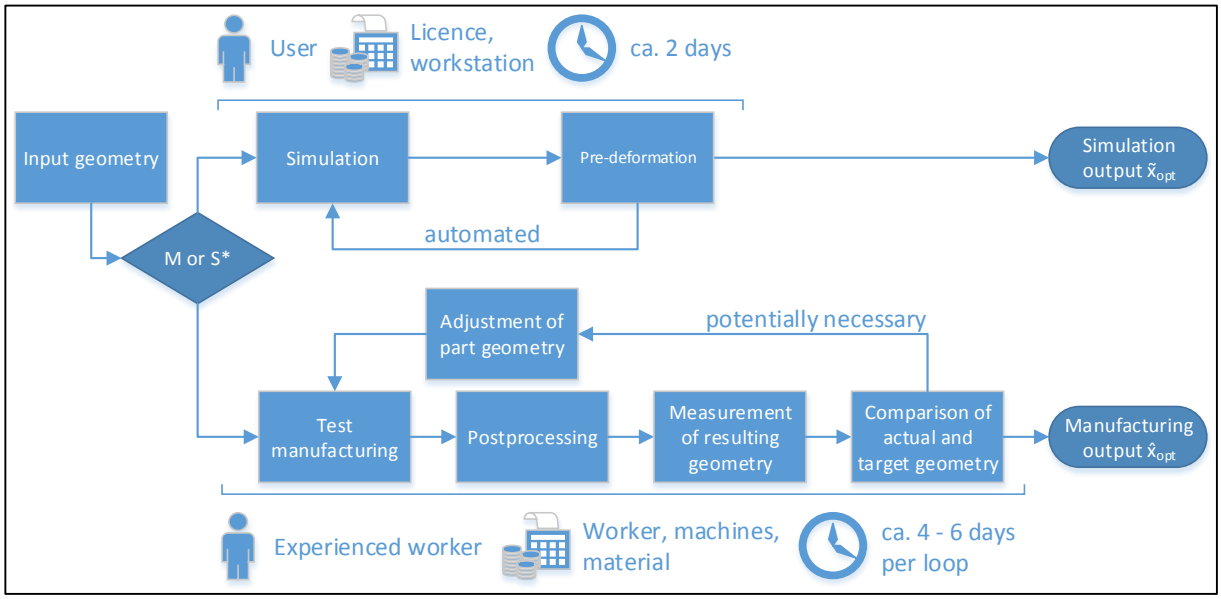

*Figure 7: Comparison of workflows for the manufacturing-based and the simulation-based process chain. Both share the initial geometry as input and an optimized geometry as output in order to manufacture a part without dimensional deviations in respect to the initial geometry. The necessary staff, the respective sources of expenses and the expected time frame are given. *M(achine-based) or S(imulation-based)*

However, the most important factor remains the quality of the results, namely the level of difference between $\hat{y}_{opt}$, $\tilde{y}_{opt}$ and y_{opt}, i. e. whether the simulation is able to correctly predict the outcome of the manufacturing process. A long-term goal is to establish a first-time-right manufacturing by use of LBM. However, simulations currently aim to accelerate the development process and support the manufacturing process. Therefore, the introduced model for the compensation of resulting warpage corresponds to a tool maturity level 3, i. e. “Material or process can be developed or assessed with significantly reduced testing. Expectation that development iterations will be reduced or eliminated. Accuracy and uncertainty effects must be quantified. Range of applicability well defined” [11].

Accordingly, future research will provide further insights into the level of agreement between the simulated and the manufactured results. An additional goal is to further decrease computational effort by developing customized simulation approaches and numerical methods.

5. Acknowledgement

The research leading to these results has received funding from the European Union's Seventh Framework Program (FP7/2007-2013) for the Clean Sky Joint Technology Initiative under grant agreement n°287087. However, explanations made reflect only the author’s views. Hence, the JU and the Union are not liable for any use that may be made of the information contained therein.

This work is based upon experiments performed at the STRESS-SPEC instrument operated by FRM II at the Heinz Maier-Leibnitz Zentrum (MLZ), Garching, Germany. Additionally, the authors would like to thank Dr. Hofmann for the constructive atmosphere during the experiments and MTU Aero Engines AG for providing CAD data and valuable feedback.

6. References

[1] Frazier, W. E.: “Metal Additive Manufacturing: A Review”, Journal of Materials Engineering and Performance, vol. 23, no. 6, 2014, pp. 1917–1928.

[2] Neugebauer, F., Keller N., Hongxiao, X., Kober, C., Ploshikhin V.: “Simulation of Selective Laser Melting Using Process Specific Layer Based Meshing”, Proc. Fraunhofer Direct Digital Manufacturing Conf.(DDMC 2014), 2014.

[3] Seidel, C., Zaeh, M. F., Wunderer, M., Weirather, J., Krol, T. A., Ott, M.: “Simulation of the Laser Beam Melting Process – Approaches for an Efficient Modelling of the Beam-material Interaction”. Procedia CIRP 25, 2014, pp. 146–153.

[4] Keller N., Ploshikhin V.: ”New method for fast predictions of residual stress and distortion of am parts”, Solid Freefrom Fabrication, 2014, pp. 1229-1237.

[5] Wu, A. S., Brown, D. W., Kumar, M., Gallegos, G. F., King, W. E.: “An experimental investigation into additive manufacturing-induced residual stresses in 316L stainless steel”, Metallurgical and Materials Transactions A, 45(13), 2014,pp. 6260-6270.

[6] Seidel, C., Wunderer, M., Zaeh, M. F., Weirather, J., Schilp, J., Slosharek, H., Graner, S., Brenner, S.: "Simulation des 3D-Druckens mittels Laserstrahlschmelzen unter Verwendung von APDL-Makro-Dateien – Potenziale und Herausforderungen“ (Hrsg.): 32. Ansys Conference & 32. CADFEM Users' Meeting, Nürnberg, 2014.

[7] Eschey, C., Feldmann, S., Zaeh, M.F.: “Rule-Based Free-Form Deformation for Additive Layer Manufacturing”, Solid Freeform Fabrication, 2011, pp. 363-374.

[8] Pottlacher, G., Hosaeus, H., Wilthan, B., Kaschnitz, E., Seifter, A.: “Thermophysikalische Eigenschaften von festem und flüssigem Inconel 718“, Thermochimica acta, 2002, pp. 255-267.

[9] Carslaw, H. S., Jaeger, J. C., “Conduction of heat in solids”, Oxford University Press, 1986

[10] Rombouts, M, Froyen, L., Gusarov, A. V., Bentefour E. H., Glorieux, C.: “Photopyroelectric measurement of thermal conductivity of metallic powders”, Journal of Applied Physicy, 2005, pp. 024905-1 - 024905-9

[11] Cowles, B., Backman, D, Dutton, R.: “Verification and validation of ICME methods and models for aerospace applications”, Integrating Materials and Manufactering Innovation, 2012, pp. 1-16

[12] Branner, G.: “Modellierung transienter Effekte in der Struktursimulation von Schichtbauverfahren”, Utz, 2011

[13] Rosenthal, D.: "Mathematical theory of heat distribution during welding and cutting." Welding journal 20.5 (1941): 220-234.